frontiers in Materials

REVIEW
published: 08 August 2019
doi: 10.3389/fmats.2019.00192

Application of Scanning Kelvin Probe in the Study of Protective Paints

Andrej Nazarov and Dominique Thierry*

French Corrosion Institute, Brest, France

Industrial coatings are composed of layers of different polymers (top coats, primers) containing pigments, corrosion inhibitors, and fillers as well as additives. For corrosion protection, it is vitally important to preserve the strong adhesion and long-term stability of the metal-polymer interface in corrosive environments. In recent decades, the performance of painted materials increased, which requires the application of advanced methods for quick assessing, ranking and predicting corrosion stability. Scanning Kelvin probe (SKP) is a highly sensitive and non-invasive technique to analyze *in situ* the metal-polymer interface of high-performance industrial coatings. SKP is able to monitor the adhesion and corrosion underneath different kinds of paints without the need for long-term corrosion tests. SKP is a localized electrochemical technique with a spatial resolution in the range of 70–100 μm. Hence, it is possible to obtain information about the intact and corroding portions of the interface at defect sites, corrosion blisters, contaminants, and intermetallics, quality of pretreatments, and the development of galvanic couples that lead to corrosion de-adhesion of the polymeric coatings. This article reviews the application of SKP to the determination of the mechanisms of corrosion de-adhesion of model paints, thick marine paints, coatings with zinc rich primers, automotive paints, and coil coatings applied on galvanized steel substrates.

Keywords: SKP, polymeric coatings, corrosion protection, adhesion, pigments, pretreatments

OPEN ACCESS

Edited by:
Michele Fedel,
University of Trento, Italy

Reviewed by:
Ole Øystein Knudsen,
Norwegian University of Science and Technology, Norway
Wolfram Fürbeth,
DECHEMA Forschungsinstitut (DFI), Germany

****Correspondence:***
Andrej Nazarov
andrej.nazarov@institut-corrosion.fr

Specialty section:
This article was submitted to Environmental Materials, a section of the journal Frontiers in Materials

Received: *28 March 2019*
Accepted: *25 July 2019*
Published: *08 August 2019*

Citation:
Nazarov A and Thierry D (2019) Application of Scanning Kelvin Probe in the Study of Protective Paints. Front. Mater. 6:192. doi: 10.3389/fmats.2019.00192

INTRODUCTION

Historically, polymeric coatings were assumed to protect the substrate from corrosion by acting as a barrier toward water, oxygen and ions. However, later studies found that oxygen and water relatively quickly saturated the coating and could not be rate determining factors in corrosion protection (Leidheiser and Granata, 1988; Thomas, 1991). Kinsella and Mayne (1969) and Mayne and Scantlebury (1970) found that ionic resistance is a key factor in polymer coating stability, known as "resistance inhibition." The relationship between the ionic resistance of a coating and its protective ability has been identified (Kinsella and Mayne, 1969; Mayne and Scantlebury, 1970). Ionic resistance has been highlighted as an important (even critical) property of a coating in modern works (Kendig and Mills, 2017; Mills and Jamali, 2017).

Funke placed great emphasis on the importance of wet adhesion to the substrate, claiming "adhesion is performance" and that it is a key factor in determining the overall coating lifetime (Funke, 1979; Negele and Funke, 1996).

The high importance placed on ionic resistance has been criticized in an article of Sykes et al. (2017). The existence of micro galvanic couples underneath the coating leads to the rapid failure of resistive coatings. Coating failure normally initiates at a local defects, which can be the result of application errors, chemical heterogeneities in the coating

or other defects, such as bubbles, under film deposits or mechanical damages. The corrosion of steel at a defect can lead to cathodic delamination of the surrounding coating (Leidheiser et al., 1983; Hamade and Dillard, 2005; Sørensen et al., 2010). On the other hand, coating de-adhesion can result from anodic undermining or filiform corrosion (Sharman, 1944; Funke, 1981). Schematics illustrating these two modes of coating de-adhesion are given in **Figure 1**. Leidheiser et al. (1983) described the mechanism for the cathodic delamination of polymeric coatings. The corrosion of steel at a defect due to the presence of an aqueous electrolyte can lead to spreading of the cathodic oxygen reduction reaction to the surrounding interface (**Figure 1A**). Delamination is effective for metals (e.g., Fe, Zn), which are covered by electron conducting surface oxide films. Considering a coated steel substrate immersed in an electrolyte at a near-neutral pH, the half-cell reaction responsible for the coating delamination process is oxygen reduction (Leidheiser et al., 1983). A linear relationship has been found between the diffusion coefficients of the different cations in an aqueous solution and the delamination rate (Leidheiser et al., 1983). The adhesion instability has been explained by the reduction of the metal oxide film at the interface or by chemical degradation of the polymer chains by products of oxygen reduction such as alkali or peroxide species. Three locus of failure have been suggested: in the oxide, in the layer of polymer or the interface (Leidheiser et al., 1983). After a weakening of the interface due to cathodic processes, residual stresses concentrated at the metal-polymer interface can cause peeling of the coating (Negele and Funke, 1996; Hamade and Dillard, 2005).

Anodic undermining or filiform corrosion has been found in polymer-coated metals exposed to humid atmospheres and is enhanced by artificial or natural impurities, such as sulfur dioxide or chloride (Sharman, 1944; Funke, 1981). It is supposed that the galvanic cell governs the growth of the filament (**Figure 1B**). Although filiform corrosion usually occurs on organic-coated aluminum parts, it has also been observed on magnesium and cold rolled steel. Filiform corrosion normally initiates at small, sometimes microscopic, scratches or defects in the coating. In the case of iron and zinc, cathodic oxygen reduction takes place at defect sites on the surface of rust, and anodic oxidation and formations $FeCl_2$ or $ZnCl_2$ develop underneath the coating prior to de-adhesion (**Figure 1B**). There is only one certain way to prevent filiform corrosion, which is to dehydrate the rusted steel surface by reducing the relative humidity of the air to below ∼60% (Funke, 1981). On the other hand, the stability of metal-paint interfaces can be enhanced by treating the metal surface, and these types of conversion coatings have a beneficial effect toward preventing filiform corrosion (Stratmann, 2005).

The electrochemical heterogeneity of the metal surface governs the spatial separation of the cathodic and anodic corrosion reactions. The stability of the coatings to corrosion driven deadhesion is determined by formation of galvanic elements and the local electrochemical methods can obtain spatially resolved information related to metal-polymer interface. The local techniques that have been applied to metals covered by organic coatings have been reviewed (Grundmeier et al., 2000; Ogle et al., 2000; Philippe et al., 2003; Stratmann, 2005; Hausbrand et al., 2008; Rossi et al., 2008; Huang et al., 2011; Upadhyay and Battocchi, 2016). A very important advantage of local scanning techniques is the possibility of comparing the map of the electrochemical parameters with the topographic information (presence of defects or rust clusters), metal microscopy data (microstructure and contaminants), differences in surface treatments, etc. DC current techniques (the scanning vibrating electrode technique and scanning electrochemical microscopy) are mainly applicable for assessing relatively low resistive paths, such as defects in the coating. Techniques based on AC current measurements (local electrochemical impedance spectroscopy and SKP) are effective for obtaining information from the interfaces underneath intact and highly resistive polymeric coatings. The objective of this particular review is to discuss the growing information concerning the application of SKP to analyze the properties of paints and paint additives that influence their stabilities and protective properties. Industrial paints have increased corrosion stabilities, and the application of highly sensitive and non-invasive *in situ* methods for quick assessment and ranking is highly important.

SKP PRINCIPLES AND APPLICATION

SKP is a non-destructive local electrochemical technique that measures the contact potential difference between a working electrode (e.g., the polymer-coated metal) and a vibrating reference electrode (e.g., a CrNi alloy or gold). A schematic of the Kelvin probe is shown in **Figure 2A**. When two metals are in contact, electrons move to reach equilibrium that creates the contact potential difference (CPD). This potential difference (ΔV, Equation 1) is proportional to the difference in the electron work functions (Φ) of the two materials. Φ is defined as the minimum work necessary to extract an electron from the Fermi level of a metal and transfer it to a point just outside the metal surface (carrying no net charge) (Hölzl and Schulte, 1979).

To measure the contact potential difference, the probe vibrates in the vertical plane, which creates a capacitor with an alternating distance, and an alternating current flows between the probe and the working electrode (Equations 2, 3). The amplitude of this current is proportional to the CPD (Equation 4).

$$\Delta V = (\Phi_w - \Phi_p)/e \quad (1)$$

$$C = \varepsilon\varepsilon^{\circ} A/(d + \Delta d \sin \omega t) \quad (2)$$

$$I(t) = I_a sin(\omega t) \quad (3)$$

$$I_a = \Delta V \varepsilon^{\circ} A\omega/d, \quad (4)$$

where e is the electron charge, C is the capacitance, ε and ε° are the dielectric constants of the surface coating and vacuum, respectively, d is the distance between the probe and working electrode, I(t) is the AC current, I_a is the amplitude of the current, ω is the frequency of the current, *t* is the time, and A is the surface area of the probe.

The work function (Φ_w, Equation 1) is a fundamental property of a metal, and it is proportional to the actual potential

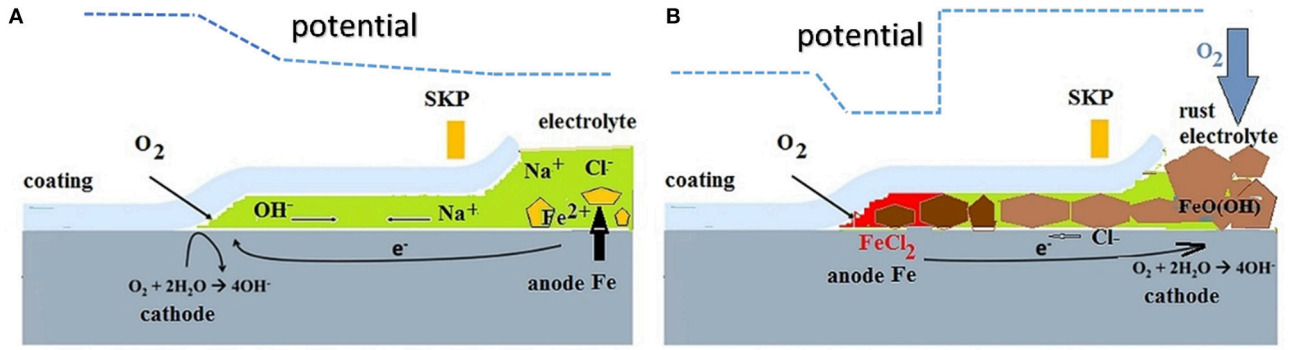

FIGURE 1 | Schematics for corrosion-driven coating de-adhesion. **(A)** Cathodic delamination and **(B)** anodic undermining galvanic cells and potential distributions along the interface.

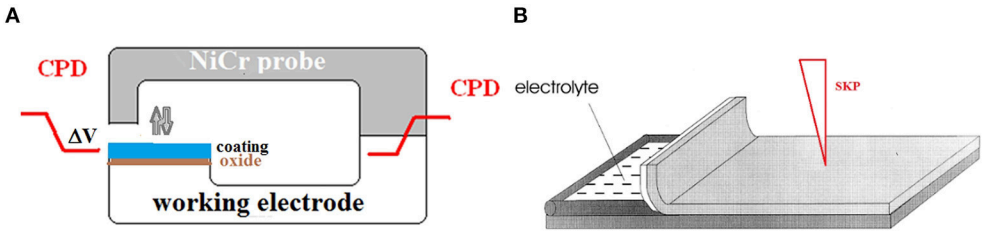

FIGURE 2 | Schematic of the Kelvin Probe **(A)** and the sketch of the sample for evaluation of cathodic delamination of a polymeric coating **(B)**.

of an electron in a metal (Equation 5; Hölzl and Schulte, 1979; Trasatti and Parsons, 1986).

$$\Phi N = -\alpha = -\mu_e + FX_w \tag{5}$$

where α is the electrochemical potential, μ_e is the chemical potential of the electrons, $\boldsymbol{N}$ and $\boldsymbol{F}$ are the Avogadro number and Faraday constant, respectively, and X_w is the potential difference across the metal-air interface (Trasatti and Parsons, 1986).

According to these definitions, the electron work function or electrochemical potential contains bulk and surface contributions. The bulk contribution is determined by the chemical potential of the electrons. The surface contribution (X_w) includes the number of potential drops related to the surface oxide film and dipole layers of adsorbed molecules (Equations 5–7).

$$X_w = \frac{\mu_{ox} - \mu_e}{e} + F_b + \beta_{ox/air} \tag{6}$$

$$X_w = \frac{\mu_{ox} - \mu_e}{e} + F_b + \beta_{ox/coating} + \beta_{coating/air} \tag{7}$$

For a bare metal surface, the potential drop (X_w, Equation 6) includes the contact potential difference between the bulk metal and oxide film relating to the difference in the corresponding chemical potentials of the electrons in the metal (μ_e) and in the oxide (μ_{ox}). The second potential drop (F_b) relates to the adsorption of environmental components (molecules of oxygen, water, etc.) that bend the conductive and valence bands of the semiconducting oxide film. The electric charges in the oxide are compensated for by the charges of the double electric layer, such as the dipoles of adsorbed species (e.g., O_2^- ions), creating a potential drop ($\beta_{ox/air}$).

For polymer-coated metals, the SKP measured potential has a potential drop (X_w, Equation 7) that includes two additional potential drops $\beta_{ox/coating}$ and $\beta_{coating/air}$. The first corresponds to charge transfer or the formation of a double electric layer of oriented dipoles between the functional groups of the polymer and the oxide that are related to the adhesive bonds (Evans and Ulman, 1990; Taylor, 2000). The second potential drop relates to the dipoles in the organic chains or charged groups of the polymer (e.g., Donnan potential drop) (Samec et al., 1993; Taylor, 2000).

Initially, the Kelvin probe was extensively applied to investigate the kinetics of metal oxidation in the gas phase, leading to the formation of oxide films. In addition, an important area of study was the adsorption of different gases onto the surface of bare metals or those covered by oxide films. These processes change the potential drop across the metal-air interface (Equation 6). Thus, CPD between a platinum probe and an evaporated metal film was monitored during the adsorption of oxygen, nitrogen or water vapor (Hackerman and Lee, 1955). Both reversible and irreversible changes of the Volta potential were found, which corresponded to the formation of either a dipole barrier or an ion barrier that prevented electron transfer. Thus, it was shown that oxygen adsorption increases the electron work function due to electron

transfer from the metal to the adsorbed oxygen molecules (Hackerman and Lee, 1955). An increase in the electron work function due to the formation of an ionic barrier related to the oxide film has also been demonstrated (Hackerman and Lee, 1955).

During measurement, the Volta potential of the probe (Φ_p/e) is kept constant. This makes possible to use CPD measurements (ΔV, Equation 1) to determine the Volta potential of the working electrode (Φ_w/e) relative to a reference electrode or determine the electron work function Φ_w relative to the vacuum level. Finally, SKP measures the surface distribution of the electrochemical potential above the metallic substrate or polymer coated metallic substrate (Grundmeier et al., 2000; Hausbrand et al., 2008). To transform Volta potential to electrochemical potential the probe has to be calibrated using a reversible reference electrode (e.g., $Cu/CuSO_4$). Modern SKP instruments measure potential distribution with a spatial resolution in the range 70–100 μm. They are equipped with an environmental chamber that enables measurements *in situ,* in a corrosive environment.

M. Stratmann and H. Streckel introduced SKP to electrochemical corrosion (Stratmann and Streckel, 1990; Frankel et al., 2007). It has been shown that for corroding metals, SKP measures the corrosion potential and can be used for studying the corrosion under very thin electrolytic films (Frankel et al., 2007). In the case of an active surface, the potential drop X_w (Equation 6) related to surface oxide significantly decreases. For metals without corrosion activators, the potential is noble and relates to the potential of the metal under passive conditions (Hausbrand et al., 2008). In this case, the redox properties of an oxide film can influence the measured potential (Grundmeier and Stratmann, 1999). According Nernst equation (Equation 8), the potential of Fe is a function of the activities of the different iron species, Fe^{3+} and Fe^{2+}, in the surface oxide:

$$\Delta E = const. + \frac{RT}{F} \ln \frac{a(Fe^{3+})}{a\left(Fe^{2+}\right)} \quad (8)$$

A potential drop in a semiconducting oxide film that does not change the oxidation state, such as in zinc, also significantly contributes to the potential measured by the SKP. An increase in the oxide thickness of a Zn/ZnO electrode increases the potential measured in air (Nazarov et al., 2015). This can be the result of an increase in the thickness of the space-charge layer in thicker oxide films. The adsorption of environmental components onto the oxide film surface also plays a role (Equations 6, 7). Replacing air with nitrogen decreased the potential of passive zinc by 100–150 mV. Thus, the formation of an oxide/O^{2-} dipole layer increased, and oxygen desorption decreased the Zn potential (Nazarov and Thierry, 2007; Nazarov et al., 2015).

Well-oxidized and uniform oxide films create stable adhesive bonds with coatings (Funke, 1979; Kendig and Mills, 2017; Mills and Jamali, 2017). The application of SKP to studies on metal surfaces are based on measuring the conditions of the surface oxide, which are characterized by a potential drop X_w (Equations 6, 7). Intermetallics, contaminations or defects in oxide locally change the potential that can be visualized by SKP (Nazarov and Thierry, 2007). Thus, SKP inspection of an oxide surface before application of polymeric coatings can detect surface defects and areas with non-uniform potential distributions, which can later lead to the formation of galvanic corrosion elements working underneath the coating and accelerating coating deadhesion.

RESULTS

SKP Assessment of Cathodic Delamination of Polymeric Coatings From Carbon and Galvanized Steels

Corrosion-driven coating de-adhesion (**Figure 1A**) is the result of a non-uniform distribution of the electrochemical potential across the metal- metal oxide -paint interface and the work of macro galvanic couples. SKP mapping of the potential makes possible to determine the galvanic elements (**Figure 1A**).

$$Fe \rightarrow Fe^{2+} + 2e \quad \text{anodic reaction} - \text{in the defect} \quad (9)$$

$$O_2 + 4e + 2H_2O \rightarrow 4OH^- \quad \text{cathodic reaction} - \text{underneath of the coating} \quad (10)$$

Using SKP, M. Stratmann et al determined the electrochemical mechanism for the cathodic delamination of polymeric coatings from steel surfaces (Stratmann et al., 1991; Leng et al., 1999a,b). SKP has the main advantage of being able to measure the potential of a metal underneath a highly resistive, intact and delaminated coating *in situ* (**Figure 1**). For measurements, an artificial defect in a coating containing a NaCl solution was prepared (**Figure 2B**). A linear relation between the coordinates for the displacement of the delamination front vs. the square root of the time of exposure was found (Leng et al., 1999a,b). These results showed that ion migration (Na^+) from the defect along the interface is the rate-controlling process for the cathodic delamination of thin model coatings (**Figure 1A**). The de-adhesion rate is determined by the mobility of the cations, but the mobility along the metal-polymer interface is much slower than the mobility of ions in the bulk electrolyte (Leng et al., 1999b). The results of SKP investigations related to cathodic delamination of the different polymeric coatings from iron, steel and galvanized steel substrates have been published in Stratmann and Hoffmann (1989), Stratmann et al. (1991), Nazarov and Thierry (1999, 2004a, 2010), Nazarov et al. (2012), Leng et al. (1999a,b), Furbeth and Stratmann (2001a,b,c), Williams and McMurray (2003), Reddy et al. (2004), Reddy and Sykes (2005), de la Fuente and Rohwerder (2008), Nazarov et al. (2012a, 2018a), and Khun and Frankel (2013).

For example, **Figure 3** shows SKP maps for alkyd coating containing TiO_2 pigment deposited on mild steel surface. The delamination starts from the scribe contaminated by NaCl aqueous electrolyte (Nazarov and Thierry, 1999). The potential of the intact interface relates to the steel in the passive state (cathode, 0.5 V vs. SHE), and at the defect site the steel has a low potential of active corrosion (anode, −0.3 to −0.2 V vs. SHE, **Figure 3**). The potential difference of 0.7 V is the electromotive force of the galvanic element leading to cathodic delamination of the coating from the defect. **Figure 4** shows typical SKP profiles

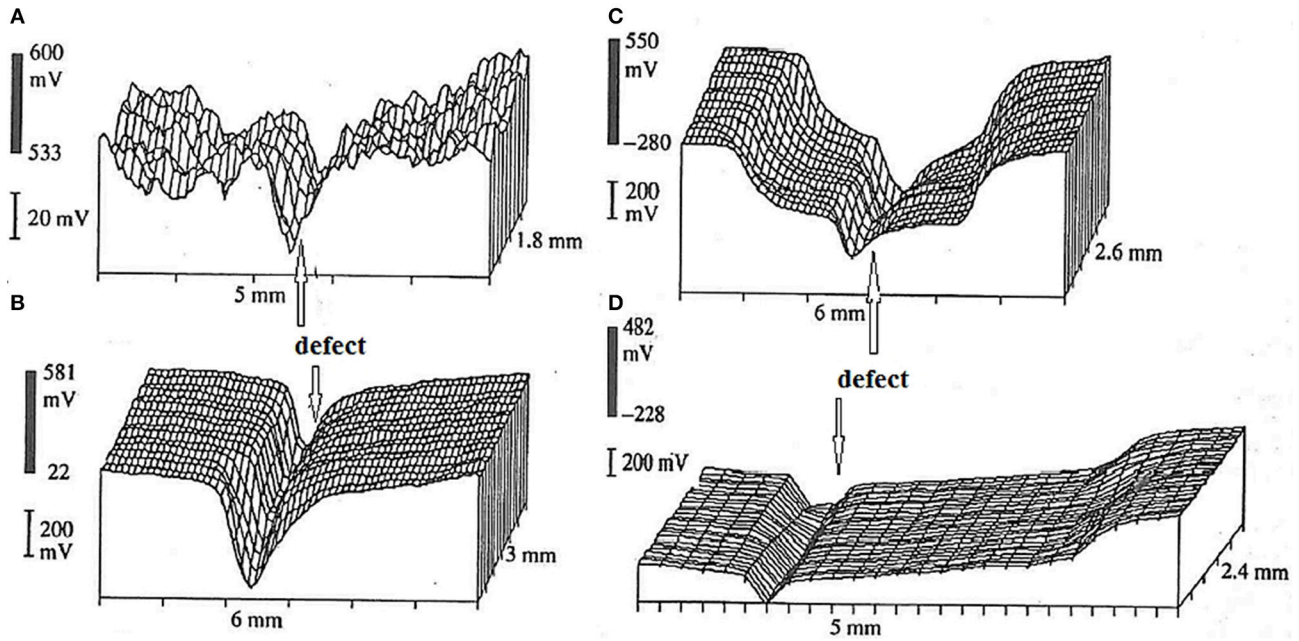

FIGURE 3 | Potential distribution (mV vs. SHE) in air at 95% RH for a carbon steel coated by alkyd coating (25 μm thick) with scribe and electrolyte 0.5 M NaCl. Before exposure **(A)**, exposure during 1 h **(B)**, 12 h **(C)**, and 24 h **(D)**. Reprinted from Nazarov and Thierry (1999) with permission.

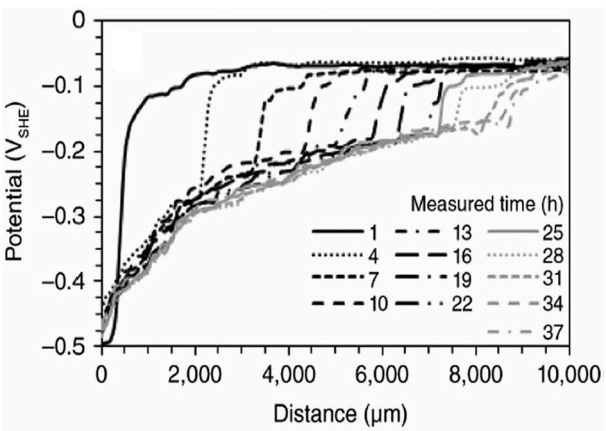

FIGURE 4 | SKP potential profiles of epoxy-coated steel sample. The exposure was carried out using 0.5 M Na_2SO_4 solution as function of distance from the defect (left hand side) for different times of exposure (Milosev and Frankel, 2018).

for steel—epoxy system as function of distance for different times of exposure in neutral 0.5 M Na_2SO_4 solution.

Other factors, such as the roughness of the steel surface and the texture of the surface, influence the cathodic delamination rate of epoxy coatings (Khun and Frankel, 2013). SKP measurements showed that an increase in the steel roughness decreased the rate of delamination. The surface features of the underlying steel substrate also influenced the cathodic delamination of the epoxy coatings. The textured lines (due to abrasion) parallel to the direction of delamination accelerated the failure compared with texture lines perpendicular to the direction of delamination. In this study, a linear dependence of the creep of coating deadhesion vs. the time of exposure was found (Khun and Frankel, 2013).

It is important to note that strong spatial separation of cathodic and anodic reactions with spreading of the cathodic reaction to the surrounding surface occurs also without a coating, due to atmospheric corrosion of steel or zinc locally contaminated by NaCl (Nazarov and Thierry, 2004a; Nazarov et al., 2015). The formation of galvanic couples consisting of anode in the region of the NaCl deposit and cathode on the bare steel surface has been observed by SKP (**Figure 5**). The distance of the cathodic spreading also had a dependence on the square root of time, and the spreading across the bare metal surface was faster compared with that of coated steel (see **Table 1**; Nazarov et al., 2018a). The electromotive force of the galvanic element that is equal to the potential difference between the low-potential anode and the noble potential of the passive steel surface was approximately 0.6 V (**Figure 5A**). This is the thermodynamic reason for galvanic corrosion. On the other hand, the rate of galvanic corrosion is a function of the rates (polarization resistances) of the partial corrosion reactions and the ionic conductivity along the interface (Nazarov and Thierry, 2004a). The area of cathodic spreading increased with increasing NaCl concentrations in the local deposits. The efficiency of the cathodic reaction on the bare steel surface governs the cathodic spreading that can be visualized by SKP (**Figure 5**). The rates of electron transfer from the substrate to oxygen molecules (Equation 10) and the migration of cations along the surface can be function of the surface chemistry. Metal surface pretreatments

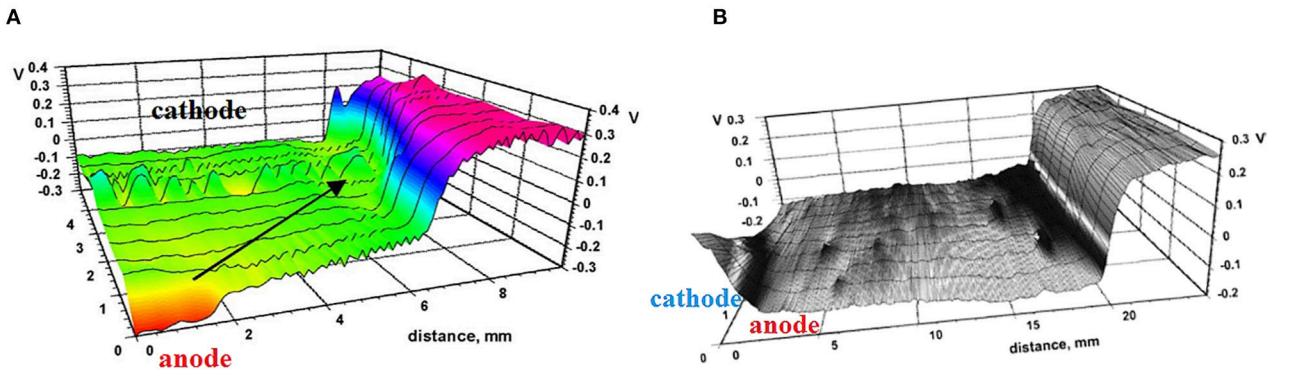

FIGURE 5 | SKP potential profile (potential in V vs. SHE) for a region of bare carbon steel surface that is locally contaminated by NaCl (left hand side), after 4 h **(A)** and 100 h **(B)** of exposure to air at 95% RH. An arrow marks the spreading of the area of cathodic reaction. Reprinted with permission from Elsevier (Nazarov and Thierry, 2004a).

TABLE 1 | Rates of cathodic deadhesion (spreading) for square root or linear kinetics during exposure in aqueous electrolytes, type of coating, and pigment, exposure conditions, coating thickness.

Coating	Exposure	Rate	Rate	Dry film thickness, μm	References
		mm/h$^{1/2}$	mm/h		
Bare steel, atmospheric corrosion	Droplet of 0.5 M NaCl	2.4		0	Nazarov et al., 2018a
Epoxy model	Aqueous electrolyte 0.5 M NaCl	1.95		40–47	Leidheiser et al., 1983
Epoxy-ester clear model	Aqueous electrolyte 0.5 M NaCl	1.2		50–60	Leng et al., 1999b
Amide-epoxy clear	Aqueous electrolyte 0.5M KCl	0.6		300	Sørensen et al., 2010
Amide epoxy pigmented flake-shaped micaceous iron oxide		0.3			
Epoxy unpigmented model	Aqueous electrolyte 3% NaCl	0.64		40	Bi and Sykes, 2011
Two layers epoxy pigmented	Aqueous electrolyte 3.5% NaCl		0.59	120–200	Bi and Sykes, 2016
Pigmented epoxy marine paint (35°C)	Aqueous electrolyte 3% NaCl		0.38	300–320	Nazarov et al., 2018a
Pigmented epoxy marine paint (22°C)	Aqueous electrolyte 3% NaCl		0.17	300–320	Nazarov et al., 2018a
Waterborne epoxy clear	Aqueous electrolyte 0.85 M NaCl	0.96		53–63	Hernández et al., 2004
Waterborne epoxy, 8.3% zinc phosphate pigment	Aqueous electrolyte 0.85 M NaCl	0.2		53–63	Hernández et al., 2004

(conversion coatings) can be ranked according to their effect on cathodic spreading. Thus, SKP measurements of bare metal surfaces can be useful for choosing the appropriate pretreatment before painting.

SKP is an ideal tool for *in situ* monitoring of the degradation processes at the buried interface contaminated by soluble salts. The study of stability of the steel/coating interfaces to initial stages of blistering and underfilm corrosion has been carried out (de la Fuente and Rohwerder, 2008; Nazarov et al., 2012a). SKP mapping gives the exact locations of the corrosion of the steel underneath a 150 μm thick layer of epoxy-diamine/polyamide paint (**Figure 6A**). This SKP study was carried out to determine the critical amount of NaCl at the interface that can prevent the development of corrosion beneath the paint. For a particular paint system, 5 μg/cm^2 was the threshold level of NaCl contamination for the paint to inhibit corrosion in humid air at 95% RH. Thus, SKP can quickly assess paints that can withstand corrosion due to NaCl contamination of the interface (de la Fuente and Rohwerder, 2008; Nazarov et al., 2012a). Corroding locations show low (active corrosion) potentials relatively surrounding intact interface (**Figure 6B**). Cathodic delamination of the coating around these active locations can be expected as the exposure time increases.

Cathodic delamination of the polymeric coating can occur on a metallic substrate that has sufficient electronic conductivity and catalytic activity to support the oxygen reduction reaction under

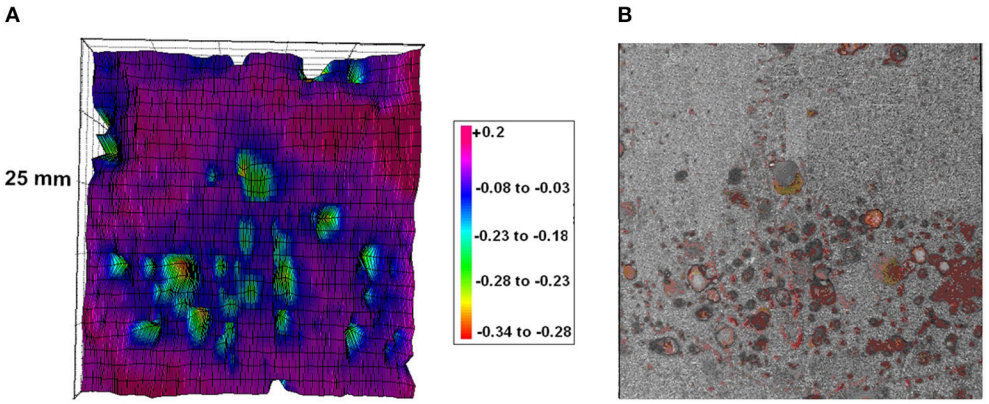

FIGURE 6 | (A) SKP map (V vs. SHE) and **(B)** the photograph of the steel surface after coating removing. The substrate was contaminated by NaCl (20 μg/cm^2). Epoxy-vinyl coating thickness 100 μm. The measurement was carried out in air at 95% RH. Reprinted with permission from NACE International (Nazarov et al., 2012a).

the coating (Leidheiser et al., 1983). Corrosion of galvanized steel in the defect down to the zinc layer leads to cathodic delamination of polymeric coatings (Furbeth and Stratmann, 2001a,b,c). The propagation kinetics of the cathodic front from the defect is proportional to the square root of the exposure time. In contrast to steel, zinc is an amphoteric metal, and the formation of alkali in cathodic region leads to the growth of an oxide layer at the zinc–polymer interface (Furbeth and Stratmann, 2001a). The cathodic reaction decreases the adhesion of a coating on a steel surface, but it completely delaminates the coating from a zinc surface.

If a defect in the organic coating is prepared through zinc layer down to the steel substrate, the polarity changes, and the defect can serve as a cathode that drives anodic coating de-adhesion from the defect. As a result, the kinetics are a complex combination of cathodic and anodic processes that occur at the metal-polymer interface (Furbeth and Stratmann, 2001b).

SKP Assessment of the Mode of Paint Corrosion Driven De-adhesion

It has been observed that the galvanic elements leading to the cathodic delamination of the coating can reverse their polarity during exposure (**Figures 1A,B**). SKP and scanning acoustic microscopy were applied to study the corrosion underneath a 120 μm thick epoxy amide resin coating (Reddy et al., 2004; Reddy and Sykes, 2005). It has been demonstrated that in some instances, the formation of iron rust at the sites of local coating degradation can reverse the potential distribution and the electrochemical activity, with rust serving as a cathodic reactant and new anodes being formed.

Thus, delamination of a thin polyvinyl butyral (PVB) coating (20 μm thick) from iron starting at a defect site containing NaCl initially showed cathodic disbondment (Williams and McMurray, 2003). Spreading of the low-potential region corresponding to delamination of the PVB coating during exposure was found. In the second phase, the formation of rust at the defect site switches the cathodic mode of de-adhesion to an anodic mode. Filaments grow from the rust locations. The rust formed on the iron underneath the coating is an effective cathodic component (Stratmann and Hoffmann, 1989). The filaments spreading either under the cathodically delaminated film or under the intact film contain low-potential active heads, where anodic iron oxidation occurs (Williams and McMurray, 2003). The heads mainly contain iron (II) chloride (**Figure 1B**). The tails of the filaments contain hydrolyzed iron-corrosion products, have a positive potential, and can serve as the cathodes in filament galvanic cells.

Contamination of the defect site in the coating by iron chloride instead of NaCl results in only anodic undermining of the coating occurring (filiform corrosion). Iron is not a mobile cation due to hydrolysis, oxidation, and rust deposition. Thus, this contaminant cannot support spreading of the cathodic region underneath the coating (Williams and McMurray, 2003).

Using steel coated by pigmented epoxy-vinyl coating (100 μm thick), it was found that the polarity of the galvanic couple and the mode of delamination were functions of the thickness of the electrolyte in the defect (Nazarov and Thierry, 2010). Under a thick electrolyte film, the defect site was anodic that polarizes the surrounding interface leading to cathodic delamination (**Figure 7A**). Under thin films, in atmospheric corrosion conditions, the defect in the same electrode showed a positive (cathodic) potential that anodically polarized the surrounding steel-coating interface and facilitated anodic undermining (**Figure 7B**). In this system, the delamination (anodic undermining) was uniform without the formation of filaments (Nazarov and Thierry, 2010). The defect and the steel underneath of the coating developed the rust with different compositions and degrees of oxidation. The anodic front (**Figure 1B** and area of low potential in **Figure 7B**) is enriched with chloride and contains $FeCl_2$. The Fe^{2+}/Fe^{3+} redox couple in the rust near the defect site provided effective cathodic oxygen reduction (Stratmann and Hoffmann, 1989).

Changes in the polarity of the galvanic elements were found for bare iron surfaces with local NaCl contaminants (Nazarov and Thierry, 2004a). Atmospheric corrosion and rust formation increased the potential of the contamination, and the potential

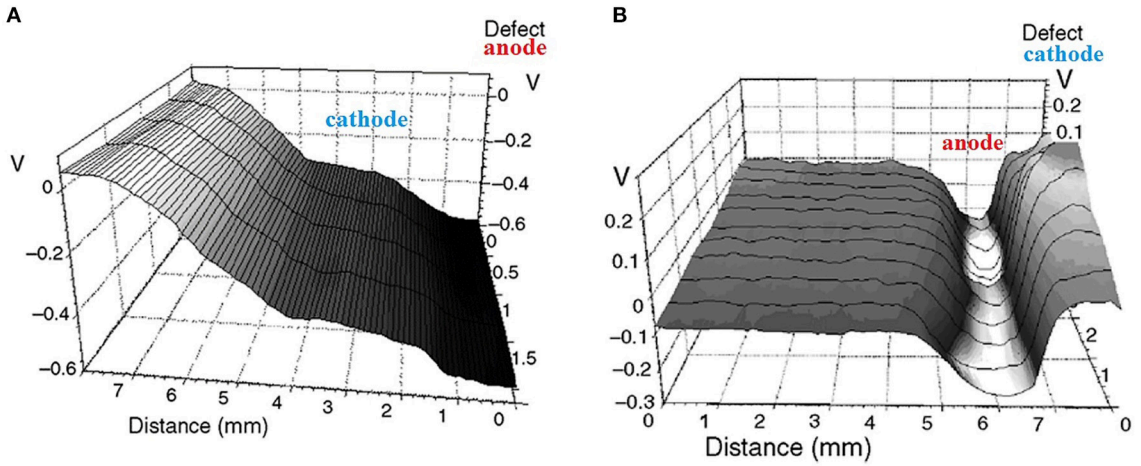

FIGURE 7 | Potential distribution (V vs. SHE) of a coated steel with a linear defect (right-hand side) in the epoxy vinyl coating (100 μm thick). **(A)** Measurement with a thick layer of aqueous electrolyte in the defect. **(B)** Measurement of the same area with a thin electrolyte layer during atmospheric corrosion at 95% RH. Reprinted with permission from NACE International (Nazarov and Thierry, 2010).

became more positive (left hand side in **Figure 5B**). However, significant anodic spreading was observed only for the coated samples. The coating additionally separates the partial reactions, creating a galvanic couple of different aeration, for which the cathode is in a well-aerated defect site and the anode is underneath the polymeric coating. For different systems, it was found that peeling out and removing the paint from anodic region transforms it into a cathodic surface (Nazarov and Thierry, 2010; Nazarov et al., 2012).

During corrosion exposures, the conditions of the defect site can periodically change, accelerating the cathodic or anodic modes of coating de-adhesion. Depending on the thickness of the electrolytic layer at the defect site, switching of the polarity of the galvanic couple was found for a polymer-coated zinc surface on a galvanized steel substrate (Nazarov et al., 2012). Using a cataphoretic epoxy coating (a system is used in the automotive industry), it was demonstrated that the potential distribution corresponded to cathodic delamination for a thick electrolytic film (**Figure 8A**) and to the anodic undermining (**Figure 8B**) in the case of atmospheric corrosion (Nazarov et al., 2012).

Only anodic de-adhesion mode, with spreading of the chloride ions and formation of anodic blisters contained $ZnCl_2$, was observed by SKP for de-adhesion of the coating from galvanized steel (Zn) from the defect down to the steel surface (Nazarov et al., 2012). A more positive steel substrate serves as a cathode, and a more negative zinc-coating interface serves as an anode. This galvanic couple governs the cut-edge corrosion of polymer coated galvanized steel (coil-coated materials) either under atmospheric or immersed in an electrolyte conditions (Nazarov et al., 2012).

Due to its low electronic conductivity, cathodic de-adhesion is strongly inhibited by substrates with dielectric oxide films, such as aluminum and magnesium alloys. However, anodic (filiform) coating de-adhesion in humid atmospheric conditions can be significant (Williams et al., 2001; Le Bozec et al., 2002; Leblanc and Frankel, 2004; Romano et al., 2009; McMurray et al., 2010).

Figure 9 shows the potential distribution over an Al alloy coated with an electrophoretic epoxy coating after 6 weeks of exposure to air at 85% RH. These systems are applied in the automotive industry. The measurements of Le Bozec et al. (2002) performed in air and argon at 95% RH showed that the exchange of the atmosphere decreased the potentials of the tail and the linear defect (**Figure 9**). Thus, pre-corroded areas of Al are a source of cathodic activity (Equation 10) directed to the anodic location in the filament head. The filament head has the potential to be more active at −0.5 V (SHE).

The stress generated during cross-linking and curing of an electrophoretic coating influences the adhesion and spreading of the filiform corrosion of an aluminum AA6016 (Romano et al., 2009). It was found that an increase in the amount of cross-linking in the epoxy cathaphoretic coating increased the adhesion and the uniform front of spreading transforms to more narrow filaments.

Finally, it is possible to point out that the mechanism of deadhesion is mainly determined by electrochemical conditions of the metal in the defect (Nazarov and Thierry, 2010). However many factors such as the electronic conductivity of the oxide film and the corrosion products, amount of water, degree of aeration, the type and concentration of pollutants are influencing and consequently only careful SKP evaluation can inform about the type of coating deadhesion and predict the coating stability under particular conditions.

SKP Assessment of Paint Stability to Delamination. Influence of Loading Pigments and Corrosion Inhibitors Into the Paints

The effects of the thickness of a polymeric film and the addition of pigments on the stability of the interface to de-adhesion have been studied using SKP. As was discussed above, the

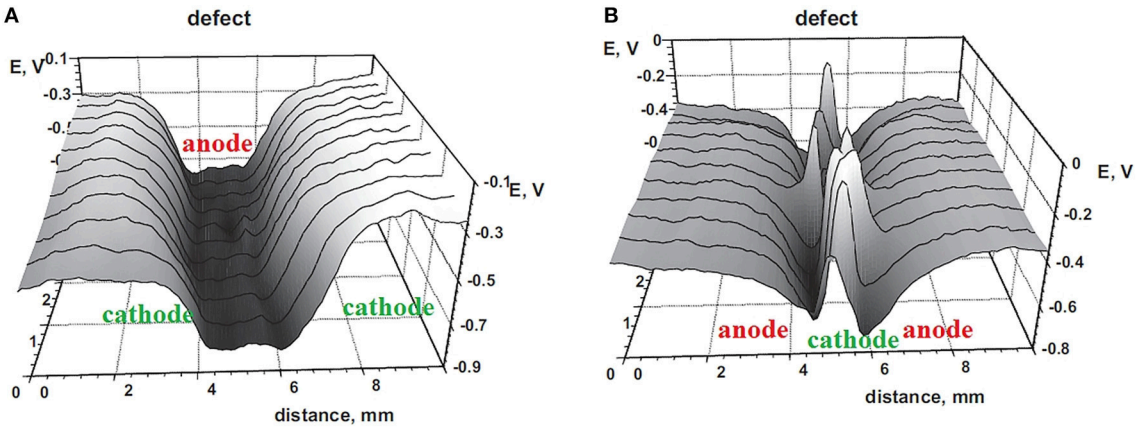

FIGURE 8 | Potential profiles (V vs. SHE) of hot-dip galvanized steel samples with linear defects in the electrophoretic epoxy coatings. Deposition of a thick electrolyte layer at the defect site **(A)** and after drying and exposing to air 95% RH **(B)**. Reprinted with permission from Elsevier (Nazarov et al., 2012).

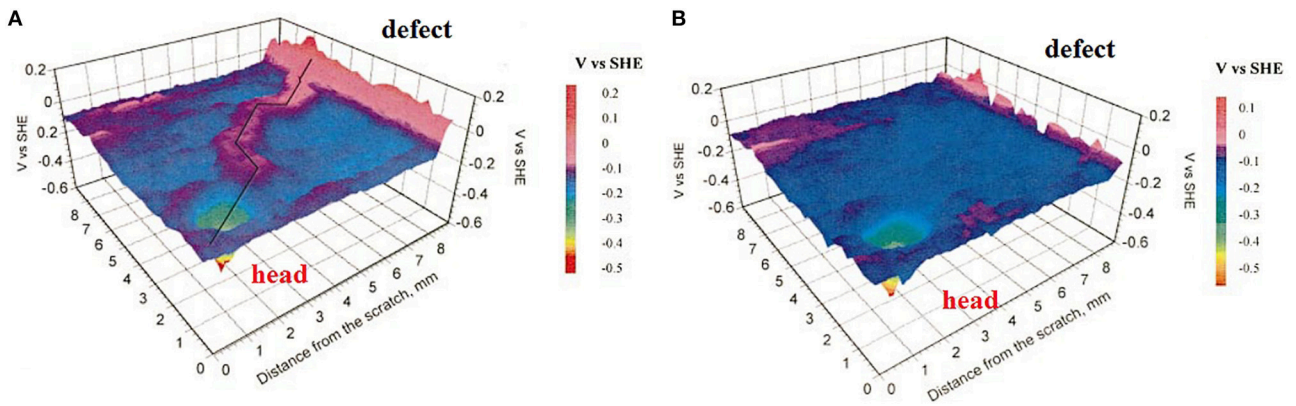

FIGURE 9 | SKP maps of the filament in electro coated AA6016 in air **(A)** and in argon **(B)** at 95% RH. Reproduced with permission from the Electrochemical Society (Le Bozec et al., 2002) Copyright 2002.

delamination rate of unpigmented coatings was controlled by cations mobility and delamination was dependent on the square root of the exposure time (Leng et al., 1999a,b; Furbeth and Stratmann, 2001c; Reddy and Sykes, 2005; Bi and Sykes, 2016). The kinetic was only slightly slower for thicker coatings (Bi and Sykes, 2016). However, the pigments can decrease the cathodic delamination rate significantly (see **Table 1**). A linear dependence of the delamination vs. time was detected for pigmented systems (Hernández et al., 2004; Grundmeier et al., 2006; Bi and Sykes, 2011, 2016; Nazarov et al., 2018a). The rate of delamination also depends from mobility of cations along the interface (Bi and Sykes, 2016). The rate of deadhesion of pigmented epoxy coatings decreased in the sequence KCl > CsCl > NaCl > LiCl (Bi and Sykes, 2016). Important parameter for pigmented coatings is number of interaction points (hydroxyl groups) between the coating and the substrate that is controlling interfacial interaction (Sørensen et al., 2010). Thus, oxygen diffusion rate, mobility of cations and adhesion are factors, which control the stability.

SKP was used to study the stability of iron with coatings contained advanced pigments based on graphene nanoplatelets and carbon nanotubes (Khun and Frankel, 2016; Glover et al., 2017, 2018). The delamination rates correlated strongly with a decrease in oxygen permeation through the coating as a function of increasing pigment volume fraction in a polyurethane/multiwalled carbon-nanotube coating (Khun and Frankel, 2016). The SKP technique was used to measure the propagation of the delamination front underneath the PVB coating. Incorporation of high-density graphene nano-platelet pigment blocked the oxygen and water pathways to the coating-steel interface, which significantly decreased the rate of cathodic delamination by 98.6% (Glover et al., 2018).

In opposite to oxygen accelerating corrosion, another air component such as carbon dioxide can decrease the corrosion rate of galvanized steel. CO_2 creates carbonates at the interface with galvanized steel during atmospheric exposure that decrease the cathodic coating delamination (Furbeth and Stratmann, 2001c). Polymeric coatings selective to CO_2 were studied. The

important work of Shkrirskiy et al. (2019) investigated the relative ability of a polymeric coating to absorb a carbon dioxide. SKP inspections showed that increased permeation of carbon dioxide through coating and access the interface is favorable for stability of coated galvanized steel (Shkrirskiy et al., 2019).

SKP was applied to study the effect chromate inhibitors that could leach from the coating (Williams and McMurray, 2001). On the other hand, in many countries, legislation does not permit the application of chromates. Less hazardous phenyl phosphonic acid was investigated as an inhibitor of corrosion-driven organic coating disbondment from iron surfaces (Glover and Williams, 2017). SKP assessment of corrosion underneath the paint was carried out *in situ* under corrosive atmospheric conditions. Increasing the loading of phosphonic acid progressively decreased the delamination rate up to 55% (Glover and Williams, 2017). From the delamination kinetics, it was concluded that the species interacting with substrate form an interfacial salt layer that inhibits oxygen reduction beneath the film and cathodic de-adhesion.

SKP was employed by the group of G. Williams and H. N. McMurray to evaluate coating delamination from Al, Fe, Zn substrates after loading of an ion-exchanger, bentonite clay (Williams and McMurray, 2004, 2017; Dodds et al., 2017). Ion exchanger supplies the interface with divalent alkali-earth and trivalent rare-earth metal cations with the subsequent precipitation of sparingly soluble hydroxides. The deposit reduced the ionic conductivity of the electrolyte underneath the polymeric coating and correspondingly decreased the current in galvanic cell. For the best performing divalent cation-exchange pigments, the inhibitory effect was comparable to or provided better protection than that of a conventional strontium chromate pigment (Williams and McMurray, 2004, 2017). Pigments containing Mg^{2+} prevented delamination of the coating from hot-dipped galvanized steel (HDG). *In situ* SKP demonstrated that the high level of inhibition of cathodic delamination could be attributed to the deposition of $Mg(OH)_2$ precipitate (Dodds et al., 2017).

SKP was applied to monitor the cathodic delamination of a 300 μm thick-pigmented epoxy coating from steel, starting from the defect site after immersion of the sample in an aqueous electrolyte (Nazarov et al., 2018a). Due to high barrier properties, this coating is applied in offshore or marine environments. It was found that at ambient temperatures, the cathodic delamination was very slow and the paint partially retained its adhesion (see **Table 1**). However, under atmospheric corrosive conditions the reduction of oxygen on the rust surface at the defect site led to rapid coating de-adhesion following the anodic undermining mechanism. Thus, anodic de-adhesion under atmospheric weathering conditions is harder to prevent compared with cathodic de-adhesion when metal-polymer joint is immersed in an electrolyte (Nazarov et al., 2018a).

Zinc-rich primers (ZRP) are components of polymeric coatings that provide active corrosion protection to steel structures in heavily corrosive environments, such as offshore. In general, a paint contains different polymeric layers with a total thickness of >400 μm that significantly delays the degradation of the paint and decreases the observation of corrosion failures. *In situ* SKP measurements of a complete paint system showed the efficiency of cathodic protection of a steel substrate by ZRP with different compositions and from different producers (Nazarov et al., 2018b). The electrolyte ingression to the interface from the defect site and activation of the Zn particles in the primer determine the ability of the primer to polarize the substrate and provided sacrificial protection under either immersed or atmospheric conditions. Thus, SKP mapping can determine the activity of the zinc particles at the interface as a function of the distance from the defect sites (scribe and cut-edge). Monitoring the interfacial potential during exposure provided information about the consumption of the zinc particles and the lifetime over which the primer could provide cathodic protection to the substrate. Thus, SKP provides a quick means of assessing the sacrificial steel protection provided by industrial marine paints containing zinc-rich primers under atmospheric or immersed conditions (Nazarov et al., 2018b).

SKP Assessment of the Metal-Metal Oxide-Coating Interface to Determine the Nature of Adhesive Bonds and Their Stability

Achieving durable corrosion protection with polymeric coatings requires an understanding of the chemical interactions at the hybrid polymer/metal oxide/metal interfaces. It is important obtain information *in situ* directly from the solid/solid interface. This section shows the possibility of SKP assessment of the metal–coating interface to determine the nature and the stability of the metal–coating bonds (Nazarov and Thierry, 2004b, 2005; Nazarov et al., 2008, 2011). Metal-polymer interactions include hydrogen bonding, ionic polar or acid-base interactions (Brönsted and Lewis kinds of interaction), and van der Waals secondary forces. Formation of the interfacial dipoles are illustrated by Equations (11) and (12) and in **Figure 10** (Nazarov and Thierry, 2004b).

$$\mathrm{OMe-OH+H-OCOR \rightarrow OMe^{+-}OCO-R+H_2O} \quad (11)$$

$$\mathrm{OMe-OH+HN-RR^{¤} \rightarrow OMeO^{-+}H_2N-RR^{¤}} \quad (12)$$

Depending on the ionic groups distributed throughout the coating, the charges in the metal and coating layers can be different. These charges can be determined by scanning across different metal-polymer joints (**Figure 10A**).

Figure 10A shows the potential distribution for steel substrate sequentially coated by alkyd and epoxy coatings. It is clear that different coatings interact with the steel surface differently. The epoxy coating significantly decreased the potentials of steel or zinc (500 mV), and the alkyd coating increased the potential (100–150 mV) (Nazarov and Thierry, 2004b, 2005). This can be explained by the formation of dipoles according to Equations (11) and (12). Alkyds contain acidic groups, and their interactions with the surface hydroxide OH-Me result in a negative charge in the coating layer and a positive charge on the metal oxide surface. Protonation of the amino groups of the epoxy coating by the OH-Me groups of the surface hydroxides creates a positive

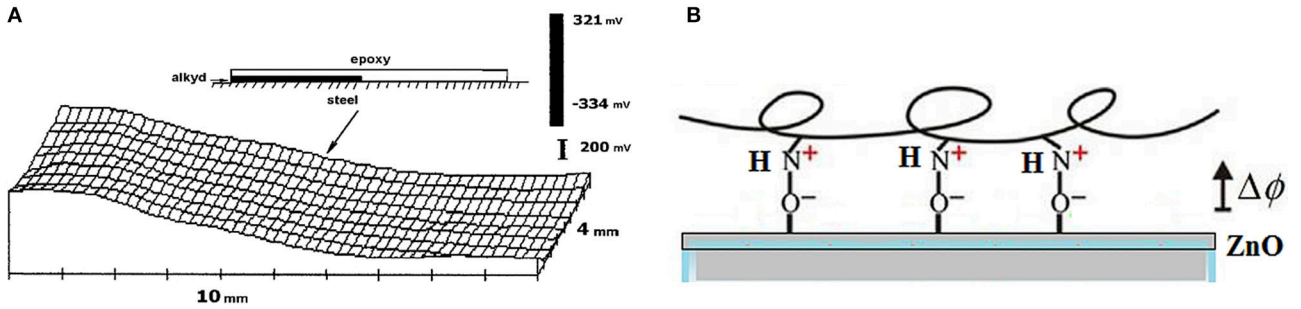

FIGURE 10 | (A) Potential distribution (mV vs. SHE) across a steel surface covered by epoxy-diamine (250 μm thick, right hand side) and alkyd coatings (35 μm thick, left hand side). Reprinted with permission from Elsevier (Nazarov and Thierry, 2004b). **(B)** Schematic of the interfacial interaction for epoxy resin.

charge in the coating and a negative charge on the metal surface (Equation 12). The potential change across the interface due to the formation of metal oxide-polymer dipoles can be illustrated by the following equation:

$$\Delta\varphi = -4\pi\alpha\mu N_S\,, \tag{13}$$

where $\Delta\varphi$ is the potential drop across the interface, N_S is the surface coverage, μ is the effective dipole moments of the adsorbed complexes, and α is polarizability (Nazarov and Thierry, 2004b, 2005; Nazarov et al., 2008).

Ingression of the water separates the interface, decreased the dipole moment and the potential drop (Equation 13), and coated surface exhibits the potential close to the values of bare metal surface (Nazarov and Thierry, 2005; Nazarov et al., 2008). However, this process is reversible, and drying the sample restores the dipoles and the initial high potential drop of coated metals with adhesive bonds (Nazarov et al., 2008). The potential changes that occur during water ingression are related to the formation of a thin aqueous film at the interface, which can lead to hydrolysis. On the other hand, a small amount of water at the interface is beneficial for increasing the degree of hydroxylation of the surface oxide (O-Me-OH) and creating anchoring hydrogen bonds that improve the interfacial durability (Nazarov et al., 2008). Aging of the samples decreased variation of the potential during wet-dry cycles and irreversibly decreased the potential drop $\Delta\varphi$ (Equation 13). Thus, the chemistry and the strength of interactions at the interface can be monitored during exposure of the adhesive joints.

Different epoxy coatings interact differently with the metal surface and create dipoles with different coverage that can be used for SKP ranking according to the adhesive force and interfacial interactions (Nazarov et al., 2011). It has been found that epoxy hardeners containing diamino groups, which are used in two-component epoxy coatings (EP1), could dissolve surface oxides (ZnO), creating stable complexes and an interphase with a mixed organic-inorganic nature. This interaction created a large potential drop across the interface and provided the highest adhesion and water stability to the metal-epoxy polymer (EP1) joint (**Figure 11A**; Nazarov et al., 2011). In contrast, another epoxy coating (EP2), which has a low adhesion to metal, showed a low potential drop (**Figure 11B**; Nazarov et al., 2011).

These points are in agreement with SKP measurements of the potential shifts of iron surfaces with adsorbed carboxylic acids, amines and amides (Wielant et al., 2008, 2010; Nazarov et al., 2011). The adsorption of amines can simulate the epoxy/amine coating systems described above. The adsorption of carboxylic acids shifted the potential in the positive direction (Equation 11), whereas adsorption of amines and amides induced a negative potential shift of 400–500 mV (Equation 12). Brönsted acid–base interactions change the overall dipole moment. The potential shift increased with the degree of protonation on the surface and increased with the amount of surface hydroxide groups (Wielant et al., 2008, 2010). These results are in line with the SKP study on the adsorption of amines and an epoxy coating on Al hydroxylated surfaces (Salgin et al., 2013b). It has been shown that the interaction of N-methyldiethanolamine in the epoxy coating with hydroxide groups on the Al surface decreased the potential of the epoxy-coated Al. The value of the potential drop could be controlled by the amount of hydroxyl groups in the oxide. In addition, the amount of interfacial dipoles can be increased by modifying the chain of an adsorbed amine with hydroxide groups (Wielant et al., 2007). Thus, the application of SKP enables new possibilities for controlling the metal-coating interface with the aim of increasing the adhesion and stability to hydrolyze of the metal-polymer bonds.

SKP Assessment of Metal Surface Pretreatments and Improvement of the Stability of the Interface to Corrosive De-adhesion

The surface energies of metallic substrates are much higher than the surface energies of polymers. This difference decreases the energy of the interfacial interactions and the stability of the contacts. Thus, we have to modify metal surfaces and create the interphases with intermediate properties to obtain good interactions with the polymer. The role of these pretreatments is to increase metal-polymer adhesion under dry and wet conditions, obtain an interface with high dielectric properties that inhibit oxygen reduction, and provide correspondingly high stability against corrosion driven delamination. In addition, the

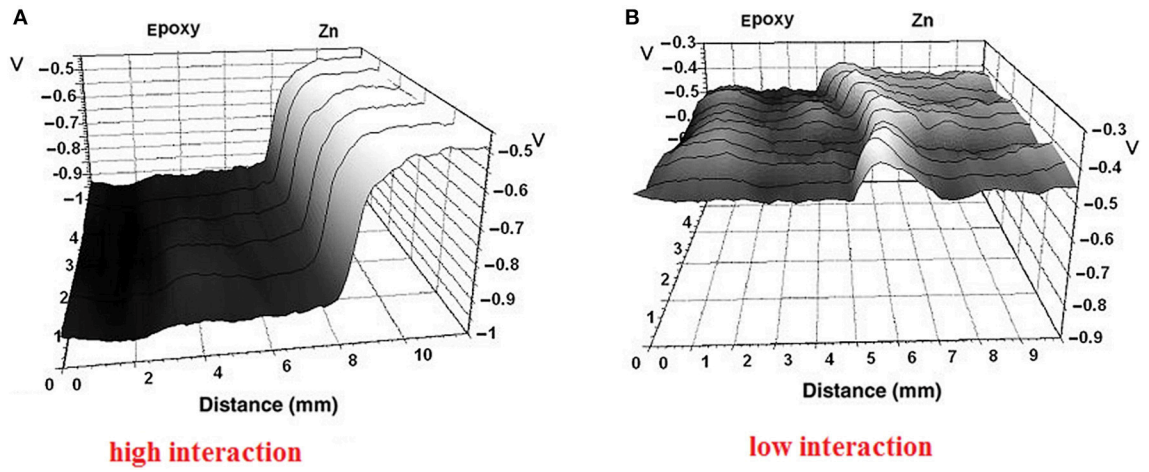

FIGURE 11 | Potential (V vs. SHE) distribution across coated and uncoated parts of zinc surface. **(A)** epoxy coating (EP1) with high interface interaction and **(B)** epoxy coating (EP2) with low interaction. Reprinted with permission from John Wiley & Sons, Ltd. Copyright 2010 (Nazarov et al., 2011).

interface has to decelerate the migration of ions along the interface, which circulate in the galvanic cells.

The correlations between the oxide surface energy of the substrate, the adhesion force of the polymer film in corrosive environments and the delamination rate from the defect site as a function of the pretreatment was shown (Wielant et al., 2009). The SKP technique has normally been used to detect the displacement of the de-adhesion front under the polymeric coating from the defect site, as discussed above. Steel surfaces were pretreated in different ways, creating surface hydroxides with different surface energies and polar components (Wielant et al., 2009). It was shown that cathodic delamination decelerates with increase of polar oxide surface energy and the adhesion interactions at the oxide-coating interface.

Additionally to adhesion, interfacial ion mobility is a key parameter in the work of surface galvanic elements on coated galvanized steel and aluminum alloy (Klimow et al., 2007; Posner et al., 2009, 2013, 2014; Salgin et al., 2013a). Cations move during the spreading of the cathodic reactions, and anions migrate across the interface during anodic undermining (**Figure 1**). The fixed surface charges (ion-exchange groups) determine the ion mobility that can be determined using SKP. Thus, controlled modification of the surface chemistry could selectively hinder or activate the mobility of the desired charge carriers to better control the electrochemical processes occurring on the oxide surface (Posner et al., 2009; Salgin et al., 2013a).

SKP can be used to study the properties of thin conversion films on steel, aluminum or galvanized steel surfaces without the deposition of a top coat. SKP was applied to phosphated zinc surfaces (galvanized steel) to study their ability to reduce oxygen in a humid atmosphere (Nazarov and Thierry, 1998). It was shown that the phosphated surfaces contaminated with carbon microparticles increased the transients of potential during exchange air to argon atmosphere. The cathodic particles were localized in the SKP maps as locations with more positive potentials relatively to the background level of phosphated zinc. Complete phosphating and replacing of the surface zinc oxide by phosphate decreased the surface potential. Thus, the potential measurements can be used for determination of the quality of phosphatation and the presence of cathodic contaminants (Nazarov and Thierry, 1998).

Investigation of the Zn/ZnO electrode using SKP (Nazarov et al., 2015) showed that cathodic spreading is effect of the semiconducting ZnO film participating in the oxygen reduction reaction. A decrease in the ZnO thickness decreased the potential of Zn and inhibited cathodic spreading. From these results, was concluded that effective pretreatment has to decrease the potential of Zn due to the formation of more dielectric and less catalytic deposits (Nazarov et al., 2005). Chromate conversion coatings have shown excellent inhibition of the corrosion. Normally, chromating creates Zn surfaces with extremely negative potentials (−0.7 V vs. SHE) (Nazarov et al., 2005). To replace chromates, different compositions have been developed, and SKP has been useful for selecting the right compositions on the base of vanadate and magnesium phosphates (Nazarov et al., 2005; Gao et al., 2018). **Figure 12** shows SKP potential transients as a result of exchanging the air atmosphere for an argon atmosphere. The magnitudes of the potential variations are proportional to the inhibition ability of the pretreated surface to adsorb and reduce oxygen. Thus, the lowest potential deviations during exchange of the atmosphere were seen in compositions containing magnesium vanadate and magnesium phosphate that were comparable with the effect of $SrCrO_4$ species (Nazarov et al., 2005). The results showed that the addition of magnesium ions was important for inhibition of oxygen reduction on the zinc surface that is in line with the studies of ion-exchange pigments leaching magnesium cations (Dodds et al., 2017; Williams and McMurray, 2017). Additionally, using SKP and XPS, V(IV) species were seen to be cathodic inhibitors of zinc corrosion. The protection was related to the formation and enrichment

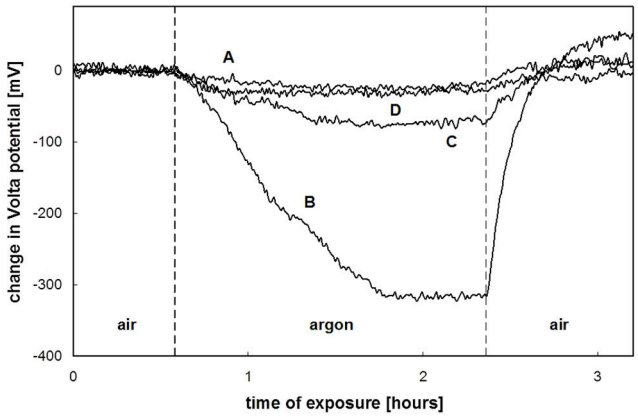

FIGURE 12 | Air-argon-air SKP potential (mV vs. SHE) transients for zinc surfaces treated with vanadate-phosphate conversion coatings. **(A)** untreated (passive), **(B)** treated in a 100 mM NaCl solution, **(C)** treated in a 100 mM NaCl solution with magnesium phosphate, **(D)** treated in the presence of magnesium vanadate, magnesium phosphate, and magnesium hydroxide in a 100 mM NaCl solution. Reproduced with permission from Nazarov et al. (2005) Copyright 2005, The Electrochemical Society.

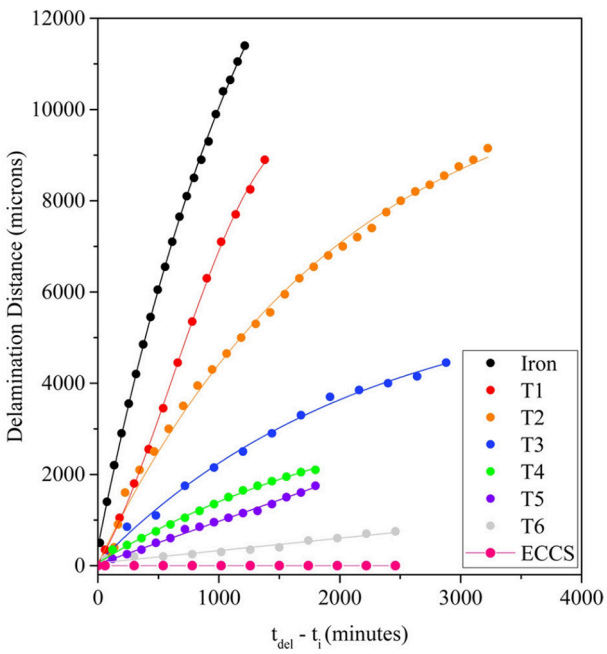

FIGURE 13 | Delamination distance vs. time of delamination of polyvinyl butyral coating on chrome-chrome oxide Cr(III)—steel substrate as function of formulation of conversion coating (Edy et al., 2019).

of the coating by V(IV) species over increasing exposure times (Gao et al., 2018).

Currently, Zr- and Ti-containing compositions were formulated to achieve better corrosion protection of zinc alloys and steels (Khun and Frankel, 2015; Lostak et al., 2016; Sababi et al., 2017; Milosev and Frankel, 2018). SKP measured the potential distribution and delamination kinetics in the vicinity of artificial defects (Milosev and Frankel, 2018). It was shown that a Zr-based treatment could decrease the electromotive force in cathodic galvanic elements and correspondingly the delamination rates of different coatings (Khun and Frankel, 2015; Lostak et al., 2016). Another silane-Zr-based conversion layers decelerated the electron transfer rate and coating delamination from galvanized steel due to the electron insulating properties of the ZrO_2 conversion coating (Lostak et al., 2016).

Important SKP works investigated the stability of polymer coated and pre-treated steels, which are applying to packaging materials (Wint et al., 2015, 2016; Edy et al., 2019). Thus, this technique was used *in situ* to compare the stability of a polyvinyl butyral coating deposited on steel substrate that was pre-coated by chromium/chromium oxide layers deposited from bath containing Cr(VI) or Cr(III) species (Wint et al., 2016). It was found that the system containing Cr (VI) species was fully resistant to all kinds of deadhesion. The conversion coating deposited from electrolyte contained Cr (III) species showed cathodic and anodic disbonding. However, cathodic delamination rate of polymeric coating pretreated by Cr (III) compositions significantly decreased after developing of the coatings (Edy et al., 2019). **Figure 13** shows the cathodic delamination rates as a function of the formulations. It was found that the conversion coating diminished electrocatalytic activity for cathodic oxygen reduction process that correlate with a decrease in the delamination rate (Edy et al., 2019). Similar SKP study of delamination of organic lacquer from tin-iron packing materials was carried out (Wint et al., 2015). It was found that tin and iron-tin intermetallics decrease the rate of cathodic oxygen reduction that also improved the coating stability to cathodic disbonding.

Surface modification of aluminum alloys is important for creating stable metal-polymer interfaces. Normally, deadhesion of the epoxy coating from an untreated Al substrate starts immediately after the ingression of water to the interface (Nazarov and Thierry, 2004b, 2005). This is the result of a low surface density of hydroxide groups in Al_2O_3, which cannot sufficiently bond with the functional groups of the coating (Salgin et al., 2013b). To solve this problem, SKP was successfully applied to find the correlations between type of Al surface modification, the density of the surface hydroxide groups and the Volta potential (Özkanat et al., 2012).

To have high stability of electrophoretic epoxy coatings on Al alloys substrates is an important issue for the automotive industry. SKP study (Nazarov et al., 2012b) compared the development of filiform corrosion as function of different sol-gel pretreatments (amino-silanes, silane-ZrO_2 (Oxsilan), and sol-gel nanoclays). It was found that some amino-silanes can accelerate anodic undermining of electrophoretic coating. Amines have a positive charge due to their protonation, which decreases the potential of the interface. After exposure, SKP found extended interfacial area that was activated by migration of the chloride ions from the defect site along the interface. Fast corrosive deadhesion of the coating can be an effect of the positive amino groups, which accelerate

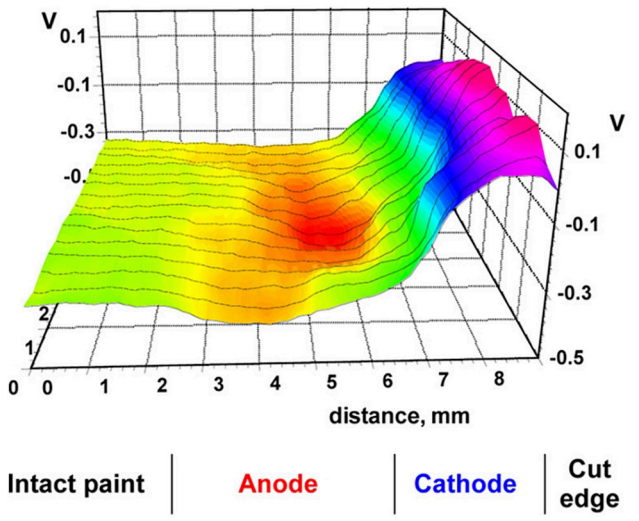

FIGURE 14 | Potential distribution (V vs. SHE) near cut edge for polymer coil coated galvanized steel panel. Reprinted with permission from Elsevier (Prosek et al., 2015).

the migration of negative chloride ions according to the ion-exchange mechanism. Other compositions decreased the area of activation and the rate of filaments spreading from the defect site (Nazarov et al., 2012b).

SKP Assessment of the Corrosion Stability of Coil Coated Hot Deep Galvanized Steels

Highly stable interface for polymer coated galvanized steel is important issue for automotive and building industries. SKP was successfully applied to study these novel Zn-Mg and Zn-Mg-Al alloys for galvanized steel with polymeric coatings (Hausbrand et al., 2003, 2009; Prosek et al., 2008, 2015; Vimalanandan et al., 2014; Davies et al., 2015). Due to the selective oxidation, the oxide film in the alloys consists of MgO, which is a perfect dielectric material and has poor electrocatalytic properties for reducing of oxygen (Prosek et al., 2008). In addition, due to the enrichment of the oxide film by MgO, the material obtains a low potential and small electromotive force for galvanic cells driving cathodic coating deadhesion (Hausbrand et al., 2009; Vimalanandan et al., 2014). Thus, alloying of zinc by Mg inhibits the cathodic delamination of polymeric coating significantly (Hausbrand et al., 2003, 2009). The strong inhibition of spreading of cathodic reaction was observed for Zn-Mg alloys with small additions of Cr, Zr, and Ti (Nazarov et al., 2017). However, Mg is remaining main component in the alloy inhibiting work of cathodic galvanic element.

Cut-edge corrosion is kind of degradation of coil coated galvanized steels. It is anodic undermining mode of coating deadhesion that is result of work galvanic element consisting from steel substrate (cathode) and the interface Zn/ZnO/polymeric coating (anode) (**Figure 14**). The electromotive force (0.4–0.5 V) between anode and cathode governs coating anodic deadhesion. Different industrial coil coatings were studied using SKP to find the effective pigments, pretreatments, composition of alloys, which decrease the rate of cut edge corrosion (Prosek et al., 2012, 2015, 2016a,b; Nazarov et al., 2017). Thus, these SKP studies were important for developing of new more corrosion stable coil coated products.

CONCLUSIONS

1. A review of the literature shows that scanning Kelvin probe is a highly effective technique for assessment of corrosion of metals underneath of dielectric polymeric coatings. Non-uniform distribution of electrochemical potential leads to work of galvanic elements and to coating deadhesion. SKP measures the potential distribution along the interface that helps to predict the coatings failure. Cathodic delamination and anodic undermining modes of corrosion driven de-adhesion can be distinguished.

2. The rate of propagation of the de-adhesion front from the defect site can be determined. The pigments in coatings decrease the rate of oxygen diffusion and inhibit cathodic disbondment. Conversion coatings, adhesion promoters and corrosion inhibitors increased the stability of an interface to anodic undermining. SKP can be used to find the effect of pretreatment on ionic conductivity along the interface controlling acceleration/deceleration effect of galvanic elements.

3. SKP is perspective technique that can determine *in situ* the nature of adhesive bonds and their stabilities. It can be used for engineering of the developed coatings and interfaces.

4. SKP technique helps quickly select most promising and long lasting protective industrial paints. The technique analyses the interface underneath the multilayer coatings *in situ*. Typically, only short-term corrosion exposure has to be employed to predict coating stability.

Thick marine paints and compositions containing zinc rich primers for marine and offshore application can be quickly ranked. Electrophoretic paints on galvanized steel or aluminum substrates used in automotive industry can be evaluated as function of curing or pretreatment chemistry. Coil coated materials used in automotive and architecture industries can be investigated in order to choose effective pretreatment, pigment and alloy composition.

AUTHOR CONTRIBUTIONS

AN was expert in application of electrochemical techniques to study corrosion and degradation of metal–polymer joints. DT was expert in theory of corrosion and electrochemistry, corrosion testing, corrosion protection by polymeric, and metallic coatings. The article was written in close collaboration.

REFERENCES

Bi, H., and Sykes, J. (2016). Cathodic delamination of unpigmented and pigmented epoxy coatings from mild steel. *Prog. Org. Coat.* 90, 114–125. doi: 10.1016/j.porgcoat.2015.10.002

Bi, H., and Sykes, J. M. (2011). Cathodic disbonding of an unpigmented epoxy coating on mild steel under semi- and full-immersion conditions. *Corros. Sci.* 53, 3416–3425. doi: 10.1016/j.corsci.2011.06.021

Davies, J. L., Glovera, C. F., Van de Langkruis, J., Zoestbergen, E., and Williams, G. (2015). The effect of Mg concentration on the resistance of PVD Zn-Mg coatings to corrosion driven organic coating delamination. *Corros. Sci.* 100, 607–618. doi: 10.1016/j.corsci.2015.08.036

de la Fuente, D., and Rohwerder, M. (2008). Fundamental investigation on the stability of the steel/coating interfaces contaminated by submicroscopic salt particles. *Prog. Org. Coat.* 61, 233–239. doi: 10.1016/j.porgcoat.2007.07.035

Dodds, P. C., Williams, G., and Radcliffe, J. (2017). Chromate-free smart release corrosion inhibitive pigments containing cations. *Prog. Org. Coat.* 102, 107–114. doi: 10.1016/j.porgcoat.2016.05.005

Edy, J. E., McMurray, H. N., Lammers, K. R., and de Vooys, A. C. A. (2019). Kinetics of corrosion-driven cathodic disbondment on organic coated trivalent chromium metal-oxide-carbide coatings on steel. *Corros. Sci*. 157, 51–61. doi: 10.1016/j.corsci.2019.04.037

Evans, S. D., and Ulman, A. (1990). Surface potential studies of alkyl-thiol monolayers adsorbed on gold. *Chem. Phys. Lett.* 170, 462–466. doi: 10.1016/S0009-2614(90)87085-6

Frankel, G. S., Stratmann, M., Rohwerder, M., Michalik, A., Maier, B., Dora, J., et al. (2007). Potential control under thin aqueous layers using a Kelvin Probe. *Corros. Sci.* 49, 2021–2036. doi: 10.1016/j.corsci.2006.10.017

Funke, W. (1979). The role of adhesion in corrosion protection by organic coatings. *J. Oil Col. Chem. Assoc*. 70, 63–75.

Funke, W. (1981). Blistering of paint films and filiform corrosion. *Prog. Org. Coat.* 9, 29–46. doi: 10.1016/0033-0655(81)80014-3

Furbeth, W., and Stratmann, M. (2001a). The delamination of polymeric coatings from electrogalvanised steel-a mechanistic approach. – Part. 1: delamination from a defect with intact zinc layer. *Corros. Sci.* 43, 207–227. doi: 10.1016/S0010-938X(00)00047-0

Furbeth, W., and Stratmann, M. (2001b). The delamination of polymeric coatings from electrogalvanized steel – a mechanistic approach. Part. 2: delamination from a defect down to steel. *Corros. Sci.* 43, 229–241. doi: 10.1016/S0010-938X(00)00048-2

Furbeth, W., and Stratmann, M. (2001c). The delamination of polymeric coatings from electrogalvanised steel – a mechanistic approach. Part. 3: delamination kinetics and influence of CO2. *Corros. Sci.* 43, 243–254. doi: 10.1016/S0010-938X(00)00049-4

Gao, Z., Zhang, D., Jiang, S., Zhang, Q., and Lia, X. (2018). XPS investigations on the corrosion mechanism of V (IV) conversion coatings on hot-dip galvanized steel. *Corros. Sci.* 139, 163–171. doi: 10.1016/j.corsci.2018.04.030

Glover, C. F., Richards, C., Baker, J., Williams, G., and McMurray, H. N. (2017). In-coating graphene nano-platelets for environmentally friendly corrosion protection of iron. *Corros. Sci.* 114, 169–172. doi: 10.1016/j.corsci.2016.11.009

Glover, C. F., Richards, C. A. J., Williams, G., and McMurray, H. N. (2018). Evaluation of multi-layered graphene nano-platelet composite coatings for corrosion control part II – Cathodic delamination kinetics. *Corros. Sci.* 136, 304–310. doi: 10.1016/j.corsci.2018.03.014

Glover, C. F., and Williams, G. (2017). Inhibition of corrosion-driven organic coating delamination and filiform corrosion on iron by phenyl phosphonic acid. *Prog. Org. Coat.* 102, 44–52. doi: 10.1016/j.porgcoat.2016.03.006

Grundmeier, G., Rossenbeck, B., Roschmann, K. J., Ebbinghaus, P., and Stratmann, M. (2006). Corrosion protection of Zn-phosphate containing water borne dispersion coatings Part. 2: Investigations of the corrosive de-adhesion of model latex coatings on iron. *Corros. Sci.* 48, 3716–3730. doi: 10.1016/j.corsci.2006.01.007

Grundmeier, G., Schmidt, W., and Stratmann, M. (2000). Corrosion protection by organic coatings: electrochemical mechanism and novel methods of investigation. *Electrochim. Acta* 45, 2515–2533. doi: 10.1016/S0013-4686(00)00348-0

Grundmeier, G., and Stratmann, M. (1999). Influence of oxygen and argon plasma treatments on the chemical structure and redox state of oxide covered iron. *J. Appl. Surf. Sci*. 141, 43–56. doi: 10.1016/S0169-4332(98)00617-5

Hackerman, N., and Lee, E. H. (1955). The effect of gases on the contact potential of evaporated metal films. *J. Phys. Chem*. 59, 900–906. doi: 10.1021/j150531a023

Hamade, R. F., and Dillard, D. A. (2005). Assessing the effects of shear, compression, and peel on the cathodic degradation of elastomer-to-metal adhesive bonds. *Int. J. Adhes. Adhes.* 25, 147–163. doi: 10.1016/j.ijadhadh.2004.06.002

Hausbrand, R., Stratmann, M., and Rohwerder, M. (2003). Delamination resistant zinc alloys: simple concept and results on the system zinc–magnesium. *Steel Res. Int*. 74, 453–458. doi: 10.1002/srin.200300212

Hausbrand, R., Stratmann, M., and Rohwerder, M. (2008). The physical meaning of electrode potentials at metal surfaces and polymer/metal interfaces: consequences for delamination. *J. Electrochem. Soc*. 155, C369–C379. doi: 10.1149/1.2926589

Hausbrand, R., Stratmann, M., and Rohwerder, M. (2009). Corrosion of zinc–magnesium coatings: mechanism of paint delamination. *Corros. Sci.* 51, 2107–2114. doi: 10.1016/j.corsci.2009.05.042

Hernández, M. A., Galliano, F., and Landolt, D. (2004). Mechanism of cathodic delamination control of zinc–aluminum phosphate pigment in waterborne coatings. *Corros. Sci.* 46, 2281–2300. doi: 10.1016/j.corsci.2004.01.009

Hölzl, J., and Schulte, F. K. (1979). "Work function of metals," in *Solid Surface Physics*, eds J. Hölzl, F. K. Schulte, and H. Wagner (Berlin; Heidelberg; New York, NY: Springer–Verlag), 9.

Huang, V. M., Wu, S. L., Orazem, M. E., Pebere, N., Tribollet, B., and Vivier, V. (2011). Local electrochemical impedance spectroscopy: a review and some recent developments. *Electrochim. Acta* 56, 8048–8057. doi: 10.1016/j.electacta.2011.03.018

Kendig, M., and Mills, D. J. (2017). An historical perspective on the corrosion protection by paints. *Prog. Org. Coat.* 102, 53–59. doi: 10.1016/j.porgcoat.2016.04.044

Khun, N. W., and Frankel, G. S. (2013). Effects of surface roughness, texture and polymer degradation on cathodic delamination of epoxy coated steel samples. *Corros. Sci.* 67, 152–160. doi: 10.1016/j.corsci.2012.10.014

Khun, N. W., and Frankel, G. S. (2015). Effect of hexafluorozirconic acid pre-treatment on cathodic delamination of epoxy coating from steel substrates. *Corrosion* 71, 277–284. doi: 10.5006/1407

Khun, N. W., and Frankel, G. S. (2016). Cathodic delamination of polyurethane/multiwalled carbon nanotube composite coatings from steel substrates. *Prog. Org. Coat.* 99, 55–60. doi: 10.1016/j.porgcoat.2016.05.002

Kinsella, E. M., and Mayne, J. E. O. (1969). Ionic conduction in polymer films I. influence of electrolyte on resistance. *Br. Polym. J.* 1, 173–176. doi: 10.1002/pi.4980010405

Klimow, G., Fink, N., and Grundmeier, G. (2007). Electrochemical studies of the inhibition of the cathodic delamination of organically coated galvanised steel by thin conversion films. *Electrochim. Acta* 53, 1291–1300. doi: 10.1016/j.electacta.2007.05.045

Le Bozec, N., Persson, D., Nazarov, A., and Thierry, D. (2002). Investigation of filiform corrosion on coated aluminium alloys by FTIR micro-spectroscopy and scanning Kelvin probe. *J. Electrochem. Soc*. 149, B403–B408. doi: 10.1149/1.1497172

Leblanc, P. P., and Frankel, G. S. (2004). Investigation of filiform corrosion of epoxy-coated. 1045 carbon steel by scanning Kelvin probe force microscopy. *J. Electrochem. Soc*. 151, B105–B113. doi: 10.1149/1.1641038

Leidheiser, H., and Granata, R. D. (1988). Ion transport through protective polymeric coatings exposed to an aqueous phase. *IBM J. Res. Dev*. 32:582. doi: 10.1147/rd.325.0582

Leidheiser, H., Wang, W., and Igetoft, L. (1983). The mechanism for cathodic delamination of organic coatings from a metal surface. *Prog. Org. Coat.* 11, 19–40. doi: 10.1016/0033-0655(83)80002-8

Leng, A., Streckel, H., and Stratmann, M. (1999a). The delamination of polymeric coatings from steel. Part. 1 Calibration of the Kelvin probe and basic delamination mechanism. *Corros. Sci.* 41, 547–578. doi: 10.1016/S0010-938X(98)00166-8

Leng, A., Streckel, H., and Stratmann, M. (1999b). The delamination of polymeric coatings from steel. Part. 2. First stage of delamination effect of type and

concentration of cations on delamination, chemical analysis of the interface. *Corros. Sci.* 41, 579–597. doi: 10.1016/S0010-938X(98)00167-X

Lostak, T., Timma, C., Krebs, S., Flock, J., and Schulz, S. (2016). Organosilane modified Zr-based conversion layer on Zn–Al alloy coated steel sheets. *Surf. Coat. Technol.* 305, 223–230. doi: 10.1016/j.surfcoat.2016.08.030

Mayne, J. E. O., and Scantlebury, J. D. (1970). Ionic conduction in polymer films II. inhomogeneous structure of varnish films. *Br. Polym. J.* 2, 240–243. doi: 10.1002/pi.4980020407

McMurray, H. N., Holder, A., Williams, G., Scamans, G. M., and Coleman, A. J. (2010). The kinetics and mechanisms of filiform corrosion on aluminium alloy AA6111. *Electrochimica Acta* 55, 7843–7852. doi: 10.1016/j.electacta.2010.04.035

Mills, D. J., and Jamali, S. S. (2017). The best tests for anti-corrosive paints. And why: a personal viewpoint. *Prog. Org. Coat.* 102, 8–17. doi: 10.1016/j.porgcoat.2016.04.045

Milosev, I., and Frankel, G. S. (2018). Review. Conversion coatings based on zirconium and/or titanium. *J. Electrochem. Soc.* 165, C127–C144. doi: 10.1149/2.0371803jes

Nazarov, A., Diler, E., Persson, D., and Thierry, D. (2015). Electrochemical and corrosion properties of ZnO/Zn electrode in atmospheric environments. *J. Electroanal. Chem.* 737, 129–140. doi: 10.1016/j.jelechem.2014.07.029

Nazarov, A., Le Bozec, N., and Thierry, D. (2018a). Assessment of steel corrosion and deadhesion of epoxy barrier paint by scanning Kelvin probe. *Prog. Org. Coat.* 114, 123–134. doi: 10.1016/j.porgcoat.2017.09.016

Nazarov, A., Le Bozec, N., and Thierry, D. (2018b). Scanning Kelvin Probe assessment of steel corrosion protection by marine paints containing Zn-rich primer. *Prog. Org. Coat.* 125, 61–72. doi: 10.1016/j.porgcoat.2018.08.024

Nazarov, A., le Bozec, N., Thierry, D., le Calve, P., and Pautasso, J.-P. (2012a). Scanning Kelvin probe investigation of corrosion under thick marine paint systems applied on carbon steel. *Corrosion* 68, 720–729. doi: 10.5006/0551

Nazarov, A., Olivier, M.-G., and Thierry, D. (2012). SKP and FT-IR microscopy study of the paint corrosion de-adhesion from the surface of galvanized steel. *Prog. Org. Coat.* 74, 356–364. doi: 10.1016/j.porgcoat.2011.10.009

Nazarov, A., Prosek, T., and Thierry, D. (2008). Application of EIS and SKP methods for the study of the zinc/polymer interface. *Electrochim. Acta* 53, 7531–7538. doi: 10.1016/j.electacta.2007.11.053

Nazarov, A., Romano, A.-P., Fedel, M., Deflorian, F., Thierry, D., and Olivier, M.-G. (2012b). Filiform corrosion of electrocoated aluminium alloy: role of the pre-treatment. *Corros. Sci.* 65, 187–198. doi: 10.1016/j.corsci.2012.08.013

Nazarov, A., and Thierry, D. (1998). Analysis of surface carbon contamination on phosphated zinc surface by scanning Kelvin probe. *J. Electrochem. Soc.* 145, L39–L42. doi: 10.1149/1.1838334

Nazarov, A., and Thierry, D. (1999). "A scanning Kelvin Probe Study of the delamination processes at the carbon steel /polymer interface," in *EFC Series, Vol. 28*, eds P. L. Bonora and F. Deflorian (London: IOM Communications), 73–78.

Nazarov, A., and Thierry, D. (2004a). Rate-determining reactions of atmospheric corrosion. *Electrochim. Acta* 49, 2717–2724. doi: 10.1016/j.electacta.2004.01.066

Nazarov, A., and Thierry, D. (2007). Application of Volta potential mapping to determine metal surface defects. *Electrochim. Acta* 52, 7689–7696. doi: 10.1016/j.electacta.2007.05.077

Nazarov, A., and Thierry, D. (2010). Influence of electrochemical conditions in a defect on the mode of paint corrosion delamination from a steel surface. *Corrosion* 66:025004-1/025004-10. doi: 10.5006/1.3319661

Nazarov, A., Thierry, D., and Prosek, T. (2017). Formation of galvanic cells and localized corrosion of zinc and zinc alloys under atmospheric conditions. *Corrosion* 73, 77–86. doi: 10.5006/2139

Nazarov, A., Thierry, D., Prosek, T., and Le Bozec, N. (2005). Protective action of vanadate at defected areas of organic coatings on zinc. *J. Electrochem. Soc.* 152, B220–B227. doi: 10.1149/1.1924067

Nazarov, A., Thierry, D., Volovitch, P., and Ogle, K. (2011). An SKP and EIS investigation of amine adsorption on zinc oxide surfaces. *Surf. Interface Anal.* 43, 1286–1298. doi: 10.1002/sia.3710

Nazarov, A. P., and Thierry, D. (2004b). Scanning Kelvin probe study of metal/polymer interfaces. *Electrochimica Acta* 49, 2955–2964. doi: 10.1016/j.electacta.2004.01.054

Nazarov, A. P., and Thierry, D. (2005). Hydrolyze of interfacial bonds in a double electric layer metal-polymer. *Prot. Metals* 41, 105–116. doi: 10.1007/s11124-005-0015-2

Negele, O., and Funke, W. (1996). Internal stress and wet adhesion of organic coatings. *Prog. Org. Coat.* 28, 285–289. doi: 10.1016/0300-9440(95)00606-0

Ogle, K., Baudu, V., Garrigues, L., and Philippe, X. (2000). Localized electrochemical methods applied to cut edge corrosion. *J. Electrochem. Soc.* 147, 3654–3660. doi: 10.1149/1.1393954

Özkanat, Ö., Salgin, B., Rohwerder, M., Mol, J. M. C., de Wit, J. H. W., and Terryn, H. (2012). Scanning Kelvin probe study of (oxyhydr)oxide surface of aluminum alloy. *J. Phys. Chem. C* 116, 1805–1811. doi: 10.1021/jp205585u

Philippe, L. V. S., Walter, G. W., and Lyon, S. B. (2003). Investigating localized degradation of organic coatings. *J. Electrochem. Soc.* 150, B111–B119. doi: 10.1149/1.1554913

Posner, R., Fink, N., Giza, G., and Grundmeier, G. (2014). Corrosive delamination and ion transport along stretch-formed thin conversion films on galvanized steel. *Surf. Coat. Technol.* 253, 227–233. doi: 10.1016/j.surfcoat.2014.05.041

Posner, R., Fink, N., Wolpers, M., and Grundmeier, G. (2013). Electrochemical electrolyte spreading studies of the protective properties of ultra-thin films on zinc galvanized steel. *Surf. Coat. Technol.* 228, 286–295. doi: 10.1016/j.surfcoat.2013.04.042

Posner, R., Wapner, K., Stratmann, M., and Grundmeier, G. (2009). Transport processes of hydrated ions at polymer/oxide/metal interfaces: Part. 1. Transport at interfaces of polymer-coated oxide covered iron and zinc substrates. *Electrochim. Acta* 54, 891–899. doi: 10.1016/j.electacta.2008.06.074

Prosek, T., Nazarov, A., Bexell, U., Thierry, D., and Serak, J. (2008). Corrosion mechanism of model zinc–magnesium alloys in atmospheric conditions. *Corros. Sci.* 50, 2216–2231. doi: 10.1016/j.corsci.2008.06.008

Prosek, T., Nazarov, A., Goodwin, F., and Šerák, J., Thierry, D. (2016a). Improving corrosion stability of Zn—Al—Mg by alloying for protection of car bodies. *Surf. Coat. Technol.* 101, 45–50. doi: 10.1016/j.surfcoat.2016.03.062

Prosek, T., Nazarov, A., Le Gac, A., and Thierry, D. (2015). Coil-coated Zn–Mg and Zn–Al–Mg: effect of climatic parameters on the corrosion at cut edges. *Prog. Org. Coat.* 83, 26–35. doi: 10.1016/j.porgcoat.2015.01.023

Prosek, T., Nazarov, A., and Stoulil, T. D. (2012). Evaluation of the tendency of coil-coated materials to blistering: field exposure, accelerated tests and electrochemical measurements. *Corros. Sci.* 61, 92–100. doi: 10.1016/j.corsci.2012.04.026

Prosek, T., Nazarov, A., Xue, H. B., Lamaka, S., and Thierry, D. (2016b). Role of steel and zinc coating thickness in cut edge corrosion of coil-coated materials in atmospheric weathering conditions; Part. 1: Laboratory study. *Prog. Org. Coat.* 99, 356–364. doi: 10.1016/j.porgcoat.2016.06.013

Reddy, B., Doherty, M. J., and Sykes, J. M. (2004). Breakdown of organic coatings in corrosive environments examined by scanning kelvin probe and scanning acoustic microscopy. *Electrochim. Acta* 49, 2965–2972. doi: 10.1016/j.electacta.2004.01.055

Reddy, B., and Sykes, J. M. (2005). Degradation of organic coatings in a corrosive environment: a study by scanning Kelvin probe and scanning acoustic microscope. *Prog. Organ. Coat.* 52, 280–287. doi: 10.1016/j.porgcoat.2004.04.004

Romano, A.-P., Olivier, M.-G., Nazarov, A., and Thierry, D. (2009). Influence of cross-linking density of a cataphoretic coating on initiation and propagation of filiform corrosion of AA6016. *Prog. Org. Coat.* 66, 173–182. doi: 10.1016/j.porgcoat.2009.06.015

Rossi, S., Fedel, M., Deflorian, F., and del Carmen Vadillo, M. (2008). Localized electrochemical techniques: theory and practical examples in corrosion studies. *C. R. Chimie* 11, 984–994. doi: 10.1016/j.crci.2008.06.011

Sababi, M., Terryn, H., and Mol, J. M. C. (2017). The influence of a Zr-based conversion treatment on interfacial bonding strength and stability of epoxy coated carbon steel. *Prog. Org. Coat.* 105, 29–36. doi: 10.1016/j.porgcoat.2016.11.016

Salgin, B., Faycal Hamou, R., and Rohwerder, M. (2013a). Monitoring surface ion mobility on aluminum oxide: effect of chemical pre-treatments. *Electrochim. Acta* 110, 526–533. doi: 10.1016/j.electacta.2013.03.060

Salgin, B., Özkanat, Ö., Mol, J. M. C., Terryn, H., and Rohwerder, M. (2013b). Role of surface oxide properties on the aluminum/epoxy interfacial bonding. *J. Phys. Chem. C.* 117, 4480–4487. doi: 10.1021/jp310121e

Samec, Z., Johnson, B. W., Capadonia, M., Jauch, M., and Dobhofer, K. (1993). Kelvin probe measurements for chemical analysis: interfacial structure of electrodes exposed to the gas phase containing water vapor. *Sens. Actuators B.* 13–14, 741–742. doi: 10.1016/0925-4005(93)85166-8

Sharman, C. F. (1944). Filiform underfilm corrosion of lacquered steel surfaces. *Nature* 153, 621–622. doi: 10.1038/153621a0

Shkrirskiy, V., Uebel, M., Maltseva, A., Lefevre, G., Volovich, P., and Rohwerder, M. (2019). Cathodic driven coating delamination suppressed by inhibition of cation migration along Zn|polymer interface in atmospheric CO_2. *npj Mater. Degrad.* 2, 2–10. doi: 10.1038/s41529-018-0064-z

Sørensen, P. A., Dam-Johansen, K., Weinel, C. E., and Kiil, S. (2010). Cathodic delamination of seawater-immersed anticorrosive coatings: mapping of parameters affecting the rate. *Prog. Org. Coat.* 68, 283–292. doi: 10.1016/j.porgcoat.2010.03.012

Stratmann, M. (2005). 2005 W.R. Whitney Award Lecture: corrosion stability of Polymer coated metals- new concepts based on fundamental understanding. *Corrosion* 61, 1115–1126. doi: 10.5006/1.3278148

Stratmann, M., and Hoffmann, K. (1989). *In situ* Möβbauer spectroscopic study of reactions within rust layers. *Corros. Sci.* 29, 1329–1352. doi: 10.1016/0010-938X(89)90123-6

Stratmann, M., and Streckel, H. (1990). On the atmospheric corrosion of metals which are covered with thin electrolyte layers. 1. verification of electrochemical technique. *Corros. Sci.* 30, 681–686. doi: 10.1016/0010-938X(90)90032-Z

Stratmann, M., Streckel, H., and Feser, R. (1991). A new technique able to measure directly the delamination of organic polymer films. *Corros. Sci.* 32, 467–470. doi: 10.1016/0010-938X(91)90126-A

Sykes, J. M., Whyte, E. P., Yu, X., and Shaher Sahir, Z. (2017). Does "coating resistance" control corrosion? *Prog. Org. Coat.* 102, 82–87. doi: 10.1016/j.porgcoat.2016.04.015

Taylor, D. M. (2000). Developments in the theoretical modelling and experimental measurements of the surface potential of condensed monolayers. *Adv. Colloid Interface Sci.* 87, 183–203. doi: 10.1016/S0001-8686(99)00044-5

Thomas, N. L. (1991). The barrier properties of paint coatings. *Prog. Org. Coat.* 19, 101–121. doi: 10.1016/0033-0655(91)80001-Y

Trasatti, S., and Parsons, R. (1986). Interphases in systems of conducting phases. *Pure Appl. Chem.* 58, 437–454. doi: 10.1351/pac198658030437

Upadhyay, V., and Battocchi, D. (2016). Localized electrochemical characterization of organic coatings: a brief review. *Prog. Org. Coat.* 99, 365–377. doi: 10.1016/j.porgcoat.2016.06.012

Vimalanandan, A., Bashir, M., and Rohwerder, M. (2014). Zn–Mg and Zn–Mg–Al alloys for improved corrosion protection of steel: some new aspects. *Mater. Corros.* 65, 392–400. doi: 10.1002/maco.201307586

Wielant, J., Hauffman, T., Blajiev, O., Hausbrand, R., and Terryn, H. (2007). Influence of the iron oxide acid–base properties on the chemisorption of model epoxy compounds studied by XPS. *J. Phys. Chem. C* 111, 13177–13184. doi: 10.1021/jp072354j

Wielant, J., Posner, R., Grundmeier, G., and Terryn, H. (2008). Interface dipoles observedafter adsorption of model compounds on iron oxide films: effect of organic functionality and oxide surface chemistry. *J. Phys. Chem. C* 112, 12951–12957. doi: 10.1021/jp802703v

Wielant, J., Posner, R., Hausbrand, R., Grundmeier, G., Terryn, H. (2009). Cathodic delamination of polyurethane films on oxide covered steel. Combined adhesion and interface electrochemical studies. *Corros. Sci.* 51, 1664–1670. doi: 10.1016/j.corsci.2009.04.014

Wielant, J., Posner, R., Hausbrand, R., Grundmeier, G., and Terryn, H. (2010). SKP as a tool to study the physicochemical interaction at buried metal-coating interfaces. *Surf. Interface Anal.* 42, 1005–10009. doi: 10.1002/sia.3512

Williams, G., and McMurray, H. N. (2001). Chromate inhibition of corrosion-driven organic coating delamination studied using a scanning Kelvin probe technique. *J. Electrochem. Soc.* 148, B377–B385. doi: 10.1149/1.1396336

Williams, G., and McMurray, H. N. (2003). The mechanism of group (I) chloride initiated filiform corrosion on iron. *Electrochem. Commun.* 5, 871–877. doi: 10.1016/j.elecom.2003.08.008

Williams, G., and McMurray, H. N. (2004). Inhibition of filiform corrosion on organic-coated AA2024-T3 by smart-release cation and anion-exchange pigments. *Corrosion*. 60, 219–228. doi: 10.5006/1.3287724

Williams, G., and McMurray, H. N. (2017). Inhibition of corrosion driven delamination on iron by smart-release bentonite cation-exchange pigments studied using a scanning Kelvin probe technique. *Prog. Org. Coat.* 102, 18–28. doi: 10.1016/j.porgcoat.2016.03.004

Williams, G., McMurray, H. N., Hayman, D., and Morgan, P. C. (2001). Time–lapse potentiometric imaging of active filiform corrosion using a scanning Kelvin probe technique. *Phys. Chem. Com.* 4, 26–31. doi: 10.1039/b100835h

Wint, N., de Vooys, A. C. A., and McMurray, H. N. (2016). The corrosion of chromium based coatings for packaging steel. *Electrochim. Acta* 203, 326–336. doi: 10.1016/j.electacta.2016.01.100

Wint, W., Geary, S., McMurray, H. N., Williams, G., de Vooys, A. C. A. (2015).The kinetics and mechanism of atmospheric corrosion occurring on tin and iron-tin intermetallic coated steels. I. cathodic delamination. *J. Electrochem. Soc.* 162, C775–C784. doi: 10.1149/2.0681514jes

Conflict of Interest Statement: The authors declare that the research was conducted in the absence of any commercial or financial relationships that could be construed as a potential conflict of interest.